One-dimensional Doppler laser collimation of chromium beam with a novel pre-collimating scheme

Baowu Zhang (张宝武), Tongbao Li (李同保), and Yan Ma (马 艳)

Department of Physics, Tongji University, Shanghai 200092

Received May 5, 2008

A novel pre-collimating scheme in laser-focused chromium (Cr) atomic deposition is presented. It consists of three apertures, which are one main pre-collimating aperture at centre and two probing apertures with uniform dimension at both sides of the central one. The calculations show that the Cr atomic beam is divided into three parts accordingly after going through this scheme, and the full-width at half-maximum (FWHM) of each part decreases while the peak value increases after one-dimensional (1D) Doppler laser collimation, subsequently. Compared with that before laser collimation, the central part does not have displacement, but each part of the other two has the same displacement to the centre after laser collimation. These phenomena which are agreed with experiment prove that the novel pre-collimating scheme is a feasible means to solve the problem which we cannot observe the collimation of Cr atomic beam after substrate in laser-focused deposition with a pre-collimating scheme of only one aperture, because the atoms will be obstructed completely by the substrate.

OCIS codes: 020.3320, 140.3320, 020.7010, 140.7010.

doi: 10.3788/COL20080610.0782.

Atom lithography[1−4] which benefits from small De Broglie wavelength of a thermal atom — typically of order 10 pm — is due to the relatively low velocity and large mass of an atom, and no resolution limit is due to Coulomb repulsion, because neutral atom offers a potential useful tool for nanostructure fabrication. The particular scheme of this technology is shown in Fig. 1. The experimental and theoretical studies of one-dimensional (1D) lines made by this technique propose a potential useful tool for nano-metrology standard[5,6].

Concerning this technique, many calculations and experiments have supported that the effect of transverse divergence of atomic beam in the XOY plane perpendicularly to the atomic beam generally dominates the limits to the minimum feature size, so the preparation of a well transverse collimated atomic beam is essential[7−11]. The technique of transverse laser cooling which utilizes a laser beam going through perpendicularly to the atomic beam, and then being retro-reflected, is usually used for this aim[12]. The fundamentals of laser cooling thoroughly described by several authors indicate that in order to well transversely collimate atomic beam, the range of transverse velocity has better to be included in about ± 3 times of the capture velocity[13]. This usually appeals to a pre-collimating scheme with only one small aperture as illustrated in Fig. 1, and works well.

Because of the importance of transverse collimation of atomic beam in atom lithography, simultaneous observation of the transverse collimation in deposition is necessary. After much work, we find that there are some difficulties to realize when using the traditional pre-collimating scheme with only one small aperture, because the atoms going through the small aperture will be obstructed completely by the substrate. In order to solve this problem, a pre-collimating scheme is presented, as shown in Fig. 2, which belongs to a new field of large pre-collimating slit in Ref. [14]. With this scheme, the atoms will be divided into three parts: the ones going through the central pre-collimating aperture B, which possess the same function to that of the aperture in traditional pre-collimating scheme, are for deposition, and the other ones going through probing aperture A and C are for indirect observation of the collimation of atoms going through aperture B after substrate in deposition. From our first typical experimental results and calculations, we find this is feasible.

The force exerting on a moving atom with transverse velocity of v_x in laser standing wave is[13]

$$F = \frac{\hbar k \Gamma}{2} \left(\frac{s_0}{1 + s_0 + 4((\delta - k v_x)/\Gamma)^2} - \frac{s_0}{1 + s_0 + 4((\delta + k v_x)/\Gamma)^2} \right), \quad (1)$$

where Γ is the natural line-width, $\hbar$ is the Planck'

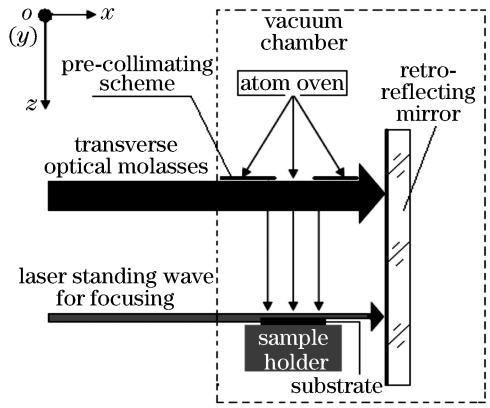

Fig. 1. Scheme of atom lithography.

 © 2008 Chinese Optics Letters

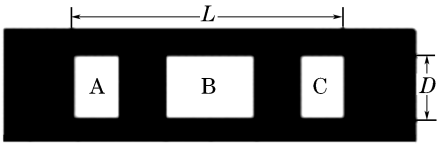

Fig. 2. Pre-collimating scheme consisting of three apertures.

constant divided by 2π, $s_0 = I/I_0$ is the on-resonance saturation parameter, which is defined by the ratio of the laser intensity I to the saturation intensity I_0 of the atomic transition, $\delta = \omega - \omega_0$ is the laser frequency ω detuning from atomic resonance frequency ω_0, and k is the laser wave vector. With the force from Eq. (1), we can obtain the equation of atomic motion,

$$m\frac{\mathrm{d}^2x}{\mathrm{d}t^2} = F(v_x), \tag{2}$$

where m is the mass of the atom, and x is the transverse coordinate. For computational convenience, we eliminate the time from Eq. (2) and get a single equation for x as a function of z which is the axial coordinate,

$$mx''(v_z)^2 = F(x' : v_z), \tag{3}$$

where x' and x'' are $\mathrm{d}x/\mathrm{d}z$ and $\mathrm{d}^2x/\mathrm{d}z^2$, respectively, v_z is the most probable longitudinal velocity, and it is a constant. With Eq. (3), using an adaptive step size, fourth-order Runge-Kutta type algorithm, we can numerically calculate laser collimation of atomic beam with the experimental parameters in Table 1. Throughout the calculation, there is no interaction among Cr atoms. For thermal Cr atomic beam, the initial transverse velocities obey Gaussian distribution, and the initial longitudinal velocities obey Maxwell-Boltzman statistics[15].

Table 1. Experimental Parameters for Simulation

Transition of Cr	$^7S_3 \rightarrow {}^7P_4^0$
Natural Line-Width Γ (MHz)	$2\pi \times 5$
Laser Wavelength λ (nm)	425.55
Laser Beam Waist in y Direction ω_y (mm)	3
Laser Beam Waist in z Direction L (mm)	24
Laser Detuning δ (MHz)	$-\Gamma$
Laser Power P (mW)	43
Temperature of Oven T (K)	1923
The Most Probable Longitudinal Velocity V_{mp} (m/s)	960
Capture Velocity V_{c} (m/s)	2.13
Initial Range of Transverse Position x (mm)	$[-0.5, 0.5]$
Initial Range of Transverse Velocity V_{x0} (m/s)	$[-21.3, 21.3]$
Distance of Pre-Collimating Scheme $L1$ (mm)	600
Distance for Observation of Collimation $L2$ (mm)	1470
Dimensions of Pre-Collimating Scheme	
$L \times D$(mm)	4.2×1
Aperture A (mm)	0.7×1
Aperture B (mm)	1.4×1
Aperture C (mm)	0.7×1

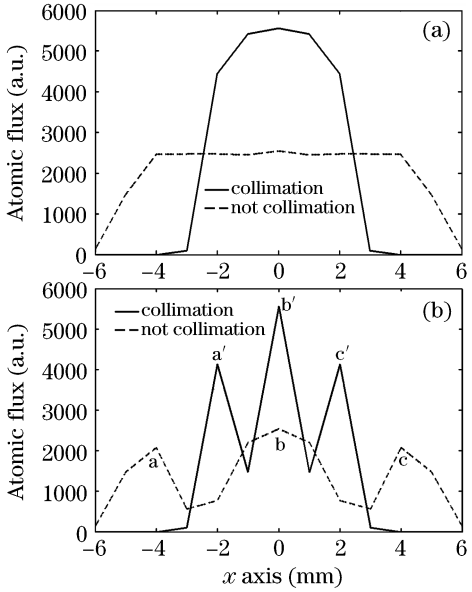

Fig. 3. Calculated distribution of the atomic beam before and after laser collimation, where (a) is that when the pre-collimating scheme is not divided ($L \times D$) and (b) is that when the pre-collimating scheme is divided into three apertures.

Table 2. Ratios of FWHM and Peak Value after Laser Collimation to that Before Collimation of Any of the Three Parts in Fig. 3(b)

Name	Ratio of Peak	Ratio of FWHM
a′/a	1.99	0.48
b′/b	2.19	0.42
c′/c	1.99	0.48

From Fig. 3 which shows the calculated distribution of the atomic beam before and after laser collimation, we can see that if the pre-collimating scheme is not divided ($L \times D$), there is only one peak at $x = 0$ with the full-width at half-maximum (FWHM) of 0.46 times and peak value of 2.19 times of those before laser collimation (Fig. 3(a)). If the pre-collimating scheme is divided into three apertures, the only one peak in Fig. 3(a) is divided into three peaks accordingly (Fig. 3(b)). They are the central one b (before laser collimation) or b′ (after laser collimation) at $x = 0$ and the other two a (before laser collimation) or a′ (after laser collimation), and c (before laser collimation) or c′ (after laser collimation) at both sides of the central one. The space between peak a (a′) and peak b (b′) is the same to that between peak c (c′) and peak b (b′). The ratios of FWHM and peak value after laser collimation to that before collimation of any of the three parts are shown in Table 2. In addition, compared with that before collimation, there is no displacement of the central peak, but uniform displacement of any of the other two to the centre after collimation.

These phenomena are agreed with experimental results shown in Figs. 4 and 5, and the experimental setup is in Ref. [14]. From Fig. 4, we can see that if the pre-collimating scheme is not divided ($L \times D$), there is only one fluorescence image either before laser collimation (Fig. 4(a)) or after laser collimation (Fig. 4(b)), and the intensity profile after laser collimation has a peak with

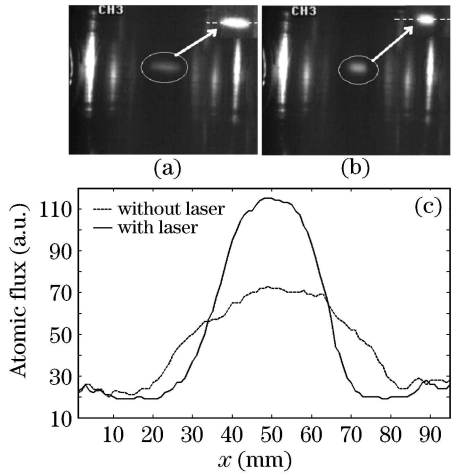

Fig. 4. Experimental results (the pre-collimating scheme is not divided). Image of fluorescence (a) before collimation and (b) after collimation; (c) the intensity profiles of the fluorescence images along the dashed lines.

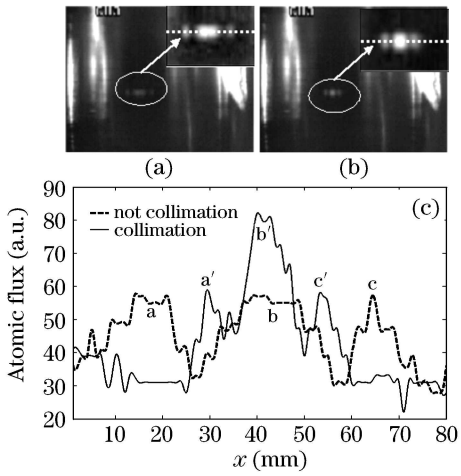

Fig. 5. Experimental results (the pre-collimating scheme is divided). Image of fluorescence (a) before collimation and (b) after collimation; (c) the intensity profiles of the fluorescence images along the dashed lines.

FWHM of 0.56 times and peak value of 1.7 times of that before laser collimation. From Fig. 5, we can see that corresponding to Fig. 2, the fluorescence image of atomic beam either before (Fig. 5(a)) or after laser collimation (Fig. 5(b)) has three parts. Compared with images before laser collimation, the image after laser collimation are brighter and shorter along the dashed lines, and the spacing between the central one and any of the other two is reduced. Figure 5(c) shows that compared with that before laser collimation (a, b, and c), the width of any of the three peaks after laser collimation (a′, b′, and c′) is shorter and the peak value is increased, and there is no displacement of the central one, but uniform displacement of any of the two sides to the centre.

In summary, our first typical theoretical and experimental results of 1D Doppler laser collimation of Cr beam with the novel pre-collimating scheme in Fig. 2 tell us that this pre-collimating scheme is a feasible tool for solution of the problem at the beginning. The atoms going through the two probing apertures present good symmetry either before or after laser collimation relative to the atomic axis, which are obstructed completely by the substrate in deposition. We can use them to indirectly observe laser collimation of the ones going through the central pre-collimating aperture B. The important notation is that this paper presents our typical results, and more work with pre-collimating schemes of different dimension to test which is the best is under way. They will appear in our later papers.

This work was supported by the National Technology Support Program of China under Grant No. 2006BAF06B08. B. Zhang's e-mail address is zhangbaowu@126.com.

References

1. C. C. Bradley, W. R. Anderson, J. J. McClelland, and R. J. Celotta, Appl. Surf. Sci. **141,** 210 (1999).
2. J. J. McClelland, R. E. Scholten, E. C. Palm, and R. J. Celotta, Science **262,** 877 (1993).
3. G. Timp, R. E. Behringer, D. M. Tennant, J. E. Cunningham, M. Prentiss, and K. K. Berggren, Phys. Rev. Lett. **69,** 1636 (1992).
4. W. Cai, C. Li, Y. Huo, and Y. Wang, Acta. Phys. Sin. (in Chinese) **48,** 611 (1999).
5. J. J. McClelland, W. R. Anderson, C. C. Bradley, M. Walkiewicz, R. J. Celotta, E. Jurdík, and R. D. Deslattes, J. Res. Natl. Inst. Stand. Technol. **108,** 99 (2003).
6. T. Li, Shanghai Measurement and Testing (in Chinese) **185,** 8 (2005).
7. J. J. McClelland, J. Opt. Soc. Am. B **12,** 1761 (1995).
8. C. Zheng, T. Li, Y. Ma, S. Ma, and B. Zhang, Acta. Phys. Sin. (in Chinese) **55,** 4528 (2006).
9. X. Chen, H. Yao, and X. Chen, Chin. Opt. Lett. **2,** 187 (2004).
10. M. Zhao, Z. Wang, Y. Ma, B. Ma, and F. Li, Chin. Opt. Lett. **5,** 602 (2007).
11. W. R. Anderson, C. C. Bradley, J. J. McClelland, and R. J. Celotta, Phys. Rev. A **59,** 2476 (1999).
12. R. E. Scholten, R. Gupta, J. J. McClelland, R. J. Celotta, M. S. Lerenson, and M. G. Vangel, Phys. Rev. A **55,** 1331 (1997).
13. H. J. Metcalf and P. van der Straten, *Laser Cooling and Trapping* (Springer-Verlag, Berlin, 1999).
14. B. Zhang, W. Zhang, Y. Ma, and T. Li, Acta. Phys. Sin. (in Chinese) **57,** 5486 (2008).
15. N. Ramsey, *Molecular Beams* (Clarendon Press, Oxford, 1956).